An Image-Based Catheter Segmentation Algorithm for Optimized Electrophysiology Procedure Workflow

Maxime Cazalas, Vincent Bismuth, and Régis Vaillant

GEHC, 283 rue de la Minière, 78533 Buc, France
Maxime.Cazalas@ge.com, Vincent.Bismuth@med.ge.com
Regis.Vaillant@med.ge.com

Abstract. Electrophysiology ablation procedures are performed in an interventional lab. The therapy is delivered through several catheters introduced in cardiac chambers under x-ray guidance. They are also be used to measure some local electrical properties which can be color-coded. A kind of color-map is then established and it can be overlaid to images of the anatomy obtained with fluoroscopy.

A potential improvement in the workflow of the procedure may be reached by tracking the location of the tip of the catheter performing the measurement. We propose here an image-based strategy to detect it and we report the results obtained on a large clinical database. We segment the object of interest by selecting contrasted objects and we characterize them by taking into account all possible co founding factors. A selection strategy has been defined from the distribution of the found values for the true positive and false positive elements in a first clinical database (3000 images from a single site). We got a success rate for the detection of the target object of 86% on a larger database formed of about 4500 images coming from 7 different sites. We also developed an active learning strategy for improving the performance of the algorithm and its stability in the field. The principle is to take into account the user's manual correction made on a given frame when processing the following ones, which is adapted to the clinical workflow: the segmentation result is assessed and corrected by an operator for each frame. We then gained additional 6% up to 91% on the success rate: the number of algorithm mistakes to be corrected by the operator is reduced to an acceptable level.

Keywords: catheter detection, ablation catheter, RF ablation, x-ray imaging, image segmentation.

1 Introduction

Electrical arrhythmia is a very common disease, which can take various forms. Some are pretty common such as left or right atrial flutter or tachycardia. A more serious form is the atrial fibrillation, the most common sustained arrhythmia, potentially leading to stroke. A classical treatment option is an invasive procedure

S. Ourselin, D. Rueckert, and N. Smith (Eds.): FIMH 2013, LNCS 7945, pp. 182–190, 2013.

involving the use of several catheters introduced in the heart chambers. Usually the catheters are navigated in the anatomy under the guidance and control of x-ray imaging. A catheter introduced in the coronary sinus delivers a time reference for the analysis of the electrical signals. Others, such as a multi-electrode catheter shaped as a ring and named lasso catheter controls the isolation of the pulmonary vein. The ablation catheter is the most important one for the procedure. It can be used either to collect electrical signal or to deliver radio-frequency energy. When employed for signal measurements, the signals are represented with a color-coded map of the anatomy. To facilitate the map creation, the location of the tip of the catheter has to be identified which is very commonly done by equipping it with an additional sensor acting like a GPS system. The cost per use of such commercial system may not be justified for procedures involving simple to treat arrhythmia or for facilities with limited budget. Supervised automatic detection of the catheter tip in x-ray fluoroscopic images may be a convenient alternative. In this image processing task, one has to cope with a number of factors: variation in the appearance of the catheter depending on its manufacturer, its model and its orientation, variation of its contrast in the image, complexity of the scene depending on the number of catheters employed in the procedure. In the following, we describe various approaches that were proposed to address similar but different problems. Indeed the previous works have focussed on different catheters whose image content are a richer set of features. We then describe the techniques that we have developed and the results obtained on a large database involving several thousands of clinical images. To the best of our knowledge, this is the first time that a systematic approach grounded in the analysis of the different sources of variation and relying on a comprehensive set of criterion is proposed and tested on a large multi-site clinical database with this objective.

2 Methods

We present here the context of the clinical problem and approaches that have been developed to address it.

2.1 Clinical Context and State of the Art

In our approach, the workflow of the procedures motivated us to segment out the catheter in each single fluoroscopic frame independently. The procedures are performed under guidance by x-ray images but the need to identify the position of the tip of the catheter is limited to a subset of the frames and the obtained location shall be validated or corrected by a technician, who shall also overlook the electrical signal. The objective is then to minimize the number of occurences requiring a manual correction.

X-ray images taken in electrophysiology ablation or mapping procedures are pretty complex because the physician introduces multiple devices in the patient's heart (see fig 1.(a)). Each of these catheters has several contrasted electrodes. The appearance of the ablation catheter is variable but it is usually one of the

most contrasted objects in the image. Its shape varies with the orientation of the catheter (see fig 1.(b)). It can be close to circular when the tip is nearly parallel to the x-ray beam. At the opposite, it is elongated when it is almost orthogonal. Right after the tip, a variable number of electrodes placed at unevenly location (see fig 3 left image) and changing from one model to the other are present. The quality of the images characterized by the amount of noise and the contrast of the different structures is also variable and depends on the patient's radiological thickness and the selected x-ray system settings.

One of the first authors [1] to publish on this topic proposed a three steps approach to detect both the tip and the catheter itself with its electrodes. The interest was also to extract the entire set of catheters. The authors tested on a limited database of about 50 images and reached a success rate of 80% for the tip, but only 38% for the entire catheter. It motivated us to focus on the tip itself. In [2,3], a correlation technique is employed to locate the catheter and the tip. Brost and al [4] have evaluated the capability of machine-learning family of algorithm for the tracking of the lasso catheter. In [5], they extend their work to two projections with an user-provided seed point to get the 3D location of the tip. So in [4], they retained a set of Haar features and Adaboost classifier. Within this family of approach, it is difficult to figure out which features are really helping for the discrimination task. So, there is no simple way to reduce the initial large number of features which may pose problem for a computer efficient implementation. Also, the characteristics of the image (new x-ray detector, different processing of the images for the display) or the characteristics of the devices may evolve along the time. In such a case, the entire process, from preparation of a database to the training of a classifier has to be done again. So with the development of a commercial product in mind, we are seeking for approaches where the impact of modifications in the image or the devices can be analyzed and integrated into the algorithm without having to collect a new full learning and test database.

We retained an approach, in the spirit of [6] whose objective was to track the catheter placed in the coronary sinus with an algorithm formed of simple steps. The main idea is to perform very carefully a first extraction of potentially relevant region of interest in the image. For each of them, we measure few parameters and link the found values with physical properties of the x-ray imaging chain or the imaged device. The distribution of the values is then evaluated for the region-of-interest corresponding to the searched device and the triggered false alarms. From this distribution, the device can be selected in the list of region-of-interest. In [6], the presence of multiple electodes eases the identification task because significantly more discriminant visual features are present.

2.2 Region-of-Interest and Parameters Extraction

The device of interest shows up as a dark structure because it attenuates more the x-ray beam than the surrounding tissue. According to the Beer-Lambert law, $I = I_0 e^{-(\mu_t + \mu_d)}$ where I_O is the x-ray incident beam, μ_t is the attenuation due to the tissue and μ_d is the incremental attenuation caused by the device. The device

can be characterized by the multiplicative factor $e^{-\mu_d}$ and the potential image without the device, i.e. the background is $I_0 e^{-\mu_t}$. To estimate the background: we do a closing with a structuring element of size superior to the estimated device size. After application of a log-transform to the initial image and to the estimated background, we subtract one image from the other. The intensity of the device in the resulting image is linked to its attenuation and shall not, in principle depends from the intensity in the background. Actually, it is not perfectly true because x-ray images are not displayed with a scale proportional to the collected x-ray beam: small contrasts are reinforced by reducing the overall dynamic of the images. Then, the contrast of the object in the displayed image varies with the anatomical background (lung, diaphragm, heart, ..). Specific corrections are necessary to retrieve the effective radio-opacity of the objects in the subtracted image. We show on fig 2(a), a clinical image, with five different catheters. The estimated background image is shown in fig 2(b) and the result of the logarithmic subtraction, where the contrasted objects from the initial image clearly show up in fig 2(c). This image is then segmented by simple thresholding and we get a set of connected components. The threshold is defined according to the typical distribution of radio-opacity of the catheters, an intrinsic property of the device. It varies only slightly with the spectrum of the x-ray beam. Typical extracted shapes are represented on the right side of fig 2(d). They are analyzed with standard shape criteria (size, eigenvalue ratio, rectangularity and average gray level in the shape).

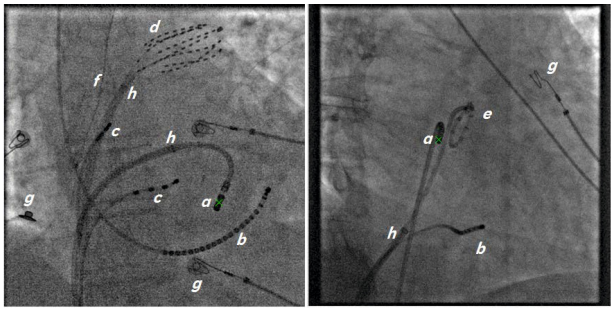

Fig. 1. Ablation catheter shape: left (right): the distal electrode of the ablation catheter is parallel (perpendicular) to the image plane. a: ablation catheter tip, b: decapolar coronary sinus catheter, c: quadripolar catheter, d: pulmonary vein basket catheter, e: pulmonary vein lasso catheter, f: esophageal temperature probe, g: surface body ECG electrode, h : transseptal sheath.

In some cases, this segmentation may combine several different items in a single object. It happens when two electrodes situated along the same catheter are not separated by the initial threshold (see fig 3). The occurrences of this situation are linked to either a small distance between the most distal electrode and the tip of the catheter or the orientation of the catheter in space with respect to the x-ray beam. Then, the distance between the two elements in the

projection is very variable. An additional treatment is applied to the largest objects. The idea is to sub-segment them into smaller objects which will then correspond to the criterion that we use to identify the tip of the catheter. For each segmented object, whose size is above a chosen parameter, the refined segmentation is obtained by applying a new threshold in the image patch including the large object. This threshold is defined from the histogram of the patch to obtain smaller objects whose size fits in the accepted range.

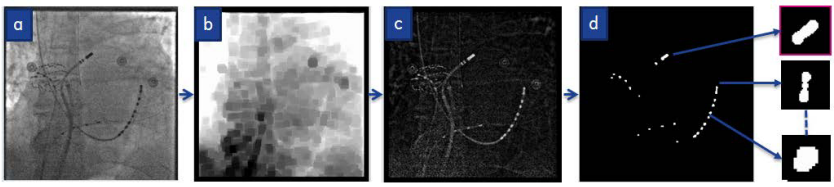

Fig. 2. Segmentation of electrodes: background image is computed with morphological closing operator. After background logarithmic subtraction, a threshold is applied and morphological operators are used to only keep catheter electrodes.

2.3 Selection of the Catheter Tip

At the end of these two first steps, about ten objects corresponding to small contrasted structure from the initial image are listed. The catheter tip has then to be selected. In our experiments, it is only in less than 1% of the cases that the tip is missing from this list. We built a decision tree based on the parameters associated to each objects i.e. size, eigenvalue ratio which indicates if the object is more or less elongated, rectangularity which measures how well the detected shape fits in a rectangle, average gray value which indicates the radio-opacity of the object.

The decision tree itself has been defined using an annotated clinical database. We have then plotted the distribution of the different parameters for the true object (i.e. the tip of the ablation catheter) and the other objects identified in the segmentation step above. An example of such distribution on the mean and eigenvalue parameters is shown in fig 4. Simple discrimination strategy such as definition of an acceptable interval on the parameter is not sufficient. Indeed, the ablation catheter may have two different appearances in the images. As shown on fig 1, it can be nearly perpendicular to the image plane and in this case, it appears as a small and very contrasted object or on contrary, it can be nearly parallel to the image plane and so appears as a more elongated and less contrasted object. The selection is based on the joint-distribution of the different couples of parameters. It is a two steps process: selection of all objects which complies with a first set of rules. The catheter tip is defined as the object with the largest intensity in this group. It may happen that this first step rejects all segmented objects. In this specific case, the list of segmented objects is filtered again with more permissive rules and the catheter tip is again chosen as the one

with the largest intensity. In some infrequent cases, we do not find any relevant item. This two steps analysis is key because we observe that the average mean is usually larger in the second one but, according to the other characteristics, the included objects are less likely to be the target.

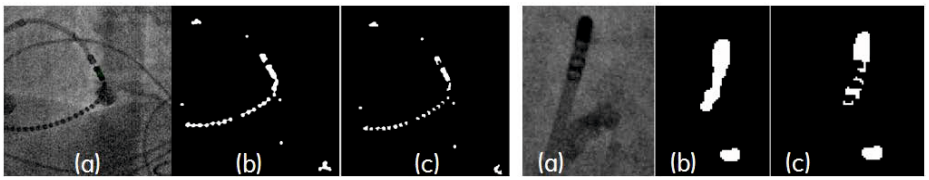

Fig. 3. Rework of the initial segmentation to sub-segment large objects in two cases: (a) original image, (b) first segmentation (c) refined segmentation

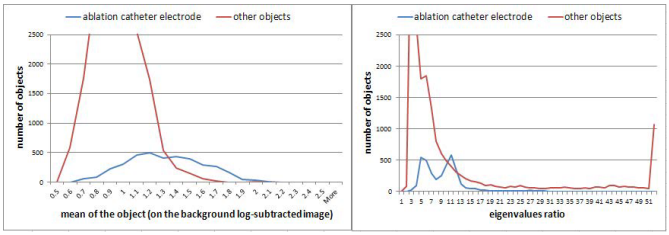

Fig. 4. Left: distribution of the object average intensity criteria; Right: distribution of the eigenvalue criteria

2.4 Active Learning Strategy

The algorithm described above is yielding encouraging results that we present in section 3 but performance seems limited. This is not surprising. As we have seen, the image may contain multiple catheters whose appearance can be similar to the ablation catheter. Moreover, the ablation catheter does not present specific and salient features that may provide strong evidence for the image-based detection. So we have to consider the impact of incorrect detections on the procedure by looking at the clinical workflow which depends on this algorithm. The procedure may last several hours. At least, two different persons are involved: a physician who is manipulating the catheters, a technician who is recording successive collected information in order to build a map of the electrical activity or to mark the location where lesions are delivered. The objective is then to limit the user interactions during the recording phase. The actions are: make sure that the catheter is properly located on the image, verify the captured electrical signal and include this information in the existing map. The algorithm shall reach a sufficient level of robustness to be more attractive than a simple identification done by the technician. The algorithm shall also avoid repetitive errors such as indicating systematically

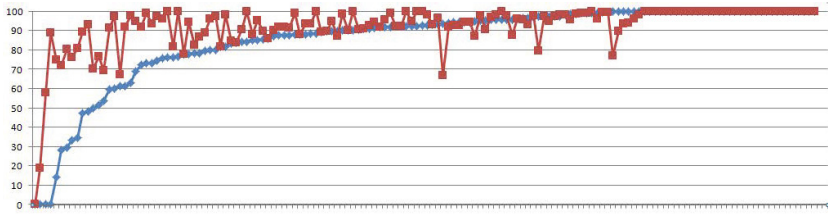

Fig. 5. Comparison of the success rate without (blue curve) and with (red curve) the use of the active learning strategy. The different runs are sorted horizontally by the success rate obtained without the active learning strategy. Vertically is the sucess rate in the run. The algorithm can be wrong for all the frames in some sequences. Then the active learning strategy brings a significant improvement.

the same erroneous position in the image. An active learning strategy was imagined as a possible way to avoid these issues. We feed the learning process with the choice made by the technician: accepts or rejects the provided location and also the chosen location in this second situation. The adopted active learning strategy is simple: the algorithm maintains a list of forbidden places i.e. image location where any potential findings of the catheter tip is a priori rejected. The list of forbidden places is formed from the location found by the algorithm and rejected. We also delete from the list the position selected by the technician. This position may not be present in the list. It may also be present because it was associated to incorrect findings in some former frames but the content may have changed. The insertion/deletion in the list of forbidden places is governed by a simple threshold on the distance in the image plane.

3 Results

To evaluate the performance of our algorithm, we built a test database of about 4 500 images, from 7 different case and 19 clinical cases There was no specific additional image acquisition, since the data collection is based on the images acquired by the physician according to his standard approach. Noisy low dose images, multiple and sometimes superimposing catheters, ... are well represented. We manually marked the tip of the catheter to establish the ground truth in all of these images.

Detection is successful when the tip is found at a distance inferior to 3 mm in the image plane from the user-defined true location. The diameter of the catheter tip is typically 2.5 mm. On this test database, we got about 85% success rate for the ablation catheter tip detection using only the image-based strategy. We also evaluated the performance with the active learning strategy described in section 2.4. The list of forbidden places was reset between cases. The modified algorithm then reached a success rate of 91%. The increase is just about 6% but it is something that may be important in some clinical cases. In some runs entirely failed because the different frames included an incorrect attractor for

the algorithm, the active learning strategy allowed to rapidly converge towards the right position (see fig 5). In [7], a success rate of 91.0% in the similar but different problem of tracking the pig-tail during a TAVI procedure is reported: large clinical databases of x-ray image include very challenging images when the radiological patient thickness is very high and the level of exposure is limited by regulatory. In these cases, the contrast is very low and algorithm fails to segment out the devices.

The algorithm implemented on a HP Z800 (4 cores 2.7GHz) computer, processes a 1000x1000 image in 90 ms.

4 Conclusion

In this work, we presented an approach to track the distal electrode of the ablation catheter during electrophysiology procedures. The algorithm uses standard image processing methods in order to segment out the contrasted objects of the image. The tip of the catheter is obtained by filtering the selected objects using quantified criteria of the segmented objects. In a systematic approach, we optimized them taking into account the specificities of the image chain and the expected object appearance in these images. This design has been evaluated against a large database of clinical images. It appears that some cases of failure due to the presence in the images of co founding elements. We have then proposed and evaluated an active learning strategy which takes into account the corrections made by the operator, who has to validate or correct the detection. With a success rate of 91%, the complete algorithm is expected to have a real added value in the clinical workflow for point-tagging during mapping or ablation procedures and is integrated to a product under development. With the active learning strategy, the operator can handle difficult imaging situations with too many devices in the field.

Even if it is not prove-out, we hope that that the design of this algorithm will support evolutions of the imaging chain characteristics (basic increased noise has already being tested through simulations) and design of the ablation catheter. At least, the impact could be evaluated by our knowledge of the internal behavior of the algorithm.

References

1. Franken, E., Rongen, P.M.P., van Almsick, M., ter Haar Romeny, B.M.: Detection of electrophysiology catheters in noisy fluoroscopy images. In: Larsen, R., Nielsen, M., Sporring, J. (eds.) MICCAI 2006. LNCS, vol. 4191, pp. 25–32. Springer, Heidelberg (2006)
2. Schenderlein, M., Dietmayer, K.: Image-based catheter tip tracking during cardiac ablation therapy. Methods, 1–5 (2010)
3. Buck, S.D., Ector, J., Gerche, A.L., Maes, F., Heidbchel, H.: Toward image-based catheter tip tracking for treatment of atrial fibrillation. In: CI2BM 2009 MICCAI Workshop on Cardiovascular Interventional Imaging and Biophysical Modelling (2009)

4. Brost, A., Liao, R., Strobel, N., Hornegger, J.: Respiratory motion compensation by model-based catheter tracking during EP procedures. Medical Image Analysis 14(5), 695–706 (2010)
5. Hoffmann, M., Brost, A., Jakob, C., Bourier, F., Koch, M., Kurzidim, K., Hornegger, J., Strobel, N.: Semi-automatic catheter reconstruction from two views. In: Ayache, N., Delingette, H., Golland, P., Mori, K. (eds.) MICCAI 2012, Part II. LNCS, vol. 7511, pp. 584–591. Springer, Heidelberg (2012)
6. Ma, Y., King, A.P., Gogin, N., Rinaldi, C.A., Gill, J., Razavi, R., Rhode, K.S.: Real-time respiratory motion correction for cardiac electrophysiology procedures using image-based coronary sinus catheter tracking. In: Jiang, T., Navab, N., Pluim, J.P.W., Viergever, M.A. (eds.) MICCAI 2010, Part I. LNCS, vol. 6361, pp. 391–399. Springer, Heidelberg (2010)
7. Wang, P., Zheng, Y., John, M., Comaniciu, D.: Catheter tracking via online learning for dynamic motion compensation in transcatheter aortic valve implantation. In: Ayache, N., Delingette, H., Golland, P., Mori, K. (eds.) MICCAI 2012, Part II. LNCS, vol. 7511, pp. 17–24. Springer, Heidelberg (2012)